Published in final edited form as:
Methods Mol Biol. 2009 ; 559: 173–190. doi:10.1007/978-1-60327-017-5_13.

Fluorometric Methods for Detection of Mitochondrial Membrane Permeabilization in Apoptosis

Soumya Sinha Roy and **György Hajnóczky**

Summary

The mitochondrial regulation of cell death involves conditions that result in the release of proapoptotic factors, such as cytochrome *c*, Smac-DIABLO, AIF, OMI/HtrA2, and others, by disruption of the outer mitochondrial membrane (OMM) permeability barrier that is controlled by pro- and antiapoptotic proteins of the Bcl-2 family. One of the mechanisms contributing to the OMM permeabilization is dependent on the interaction of proapoptotic Bcl-2 family proteins and other factors straight with the OMM. Another mechanism is initiated by the permeability transition of the inner mitochondrial membrane (IMM), leading to an increase in the matrix volume and reorganization of the IMM structure, which in turn, influence the OMM permeability barrier. The OMM also provides surface for the assembly of the apoptosome, where the mitochondria-derived proapoptotic factors induce caspase activation. Fluorescence measurements have been devised for evaluation of the barrier function of both OMM and IMM and of the downstream effectors of the factors released from the mitochondria to the cytosol. Many of these measurements are real-time, quantitative, and can be conveniently performed in a fluorometer cuvette containing suspensions of permeabilized cells or isolated mitochondria. This chapter provides a step-by-step manual for the measurements of the mitochondrial membrane potential, retention of Ca^{2+} and cytochrome *c*, matrix volume, and caspase activation and discusses protocols for discrimination between different mechanisms of the OMM permeabilization.

Keywords

Apoptosis; Mitochondrial membrane permeability; Fluorometer; Mitochondrial membrane potential; Western blot

1. Introduction

The number of studies concerned with mitochondria and apoptosis showed a progressive rise in the past 15 years. Mitochondria were recognized first as the main source of cellular ATP production, but over recent years their role has also been established in many aspects of cell physiology and pathophysiology (1). For example, to regulate cell survival, mitochondria participate in calcium signaling by rapidly accumulating and releasing Ca^{2+} and retain proteins that induce execution of apoptosis upon release to the cytosol (2). Initiation of the mitochondrial pathway of apoptosis signaling results in the permeabilization of the outer mitochondrial membrane (OMM) and the release of proapoptotic mitochondrial proteins which are mainly the residents of intermembrane space (IMS) (3, 4). Presently, there are two recognized mechanisms for the OMM permeabilization (Fig. 1). The first involves the opening of the permeability transition pore (PTP) that seems to be a multiprotein complex localized at the contact sites of the OMM and inner mitochondrial membrane (IMM). Activation of the PTP permits the flux of ions and solutes between the

matrix space and the extramitochondrial space, leading to dissipation of the membrane potential, loss of the ATP production, pH gradient, and gradual expansion of the matrix volume. Reorganization of the cristae allows matrix swelling without rupture of the IMM, but the OMM cannot accommodate to a large increase in volume and therefore prone to break. Notably, PTP opening may initiate cytochrome *c* release in the absence of large scale matrix swelling and permanent metabolic impairments in some conditions, raising the possibility that an alternative mechanism may also couple reversible PTP opening to the permeabilization of the OMM. Based on early biochemical studies, the PTP was envisioned as a complex formed by the voltage-dependent anion channel (VDAC), adenine nucleotide translocator (ANT), and mitochondrial cyclophilin D (CypD). Recent genetic studies have reported that the knockout of any ANT isoforms or VDAC isoforms or CypD does not affect or only evokes a quantitative change in the activation of the PTP, arguing for the involvement of some other factors in the formation of the pore (5). The PTP activation is usually triggered by mitochondrial Ca^{2+} uptake and the ensuing rise in mitochondrial matrix $[Ca^{2+}]$ ($[Ca^{2+}]_m$) and/or by reactive oxygen species (ROS) (6). However, other factors, including pH, $\Delta\Psi_m$, Bcl-2/xL, and adenine nucleotides also modulate the PTP opening. These factors synergize with each other in PTP activation and receive input from a variety of signaling molecules such as ceramide or arachidonic acid (7, 8).

The second mechanism of OMM permeabilization is induced by a proapoptotic protein of the Bcl-2 family, such as Bax or Bid. Bcl-2 family proteins play a fundamental role in the integration of proapoptotic and antiapoptotic signals and many of those proteins are localized to and control the permeability properties of intracellular membranes (9–11). Among the proapoptotic Bcl-2 family proteins, Bak and a small fraction of Bax are associated with the mitochondria, whereas several BH3-only proteins, e.g., Bid and the major part of Bax are in the cytoplasm of surviving cells, but exhibit redistribution to the mitochondria during apoptosis. Oligomerization of OMM-integrated Bax and Bak is thought to contribute to the formation of a pore upon apoptotic insult, which permits the release of proapoptotic mitochondrial proteins from IMS (12). In response to engagement of the death receptors Bid is cleaved by activated caspase-8, and subsequently, the truncated C-terminus Bid (tBid) is translocated from cytoplasm to the mitochondria. After translocation to the OMM, tBid either directly activates oligomerization of Bax and Bak to form a pore or antagonizes their antiapoptotic counterparts (Bcl-2, Bcl-xl, etc.) and indirectly helps oligomerization of Bax and Bak (13, 14).

Only a smaller fraction of the IMS is in the peripherial IMS and the majority of the proteins are compartmentalized in the cristae. Evidence has been presented that the release of the IMS proteins from the cristae requires opening and reorganization of the cristae (15).

The following subheadings describe methods for the study of the mitochondrial phase of apoptosis using a fluorometer and different fluorescent dyes in suspensions of permeabilized cells. The evaluated parameters are marked in Fig. 1 (italics).

2. Materials

2.1. Cell Culture

1. Human hepatoma cell line HepG2 (ATCC) and rat cardiac muscle cell line H9c2 (ATCC).
2. Dulbecco's Modified Essential Medium (DMEM) supplemented with 10% fetal bovine serum (Gibco).
3. Sodium pyruvate (Gibco), L-glutamine (Biowhittaker) and Penicillin/Streptomycin (10,000 U/mL and 10,000 μg/mL, respectively) (Biowhittaker).

4. Trypsin (0.25%) and EDTA (1 mM) (Gibco).
5. tBid (Serono Pharmaceutical).

2.2. Assay Buffers

1. Ca^{2+} free extracellular buffer (Na-HEPES-EGTA): 120 mM NaCl, 5 mM KCl, 1 mM KH_2PO_4, 0.2 mM $MgCl_2$, 0.1 mM EGTA, 20 mM HEPES–NaOH pH 7.4.
2. Intracellular medium (ICM): 120 mM KCl, 10 mM NaCl, 1 mM KH_2PO_4, 5% Dextran, 20 mM HEPES–Tris pH 7.2 supplemented with 1 μg/mL of each of antipain, leupeptin, and pepstatin (Sigma). For Ca^{2+} measurement ICM was passed through a Chelex column (Chelex 100 resins) (Bio-Rad) prior to addition of protease inhibitors to lower the ambient [Ca^{2+}].
3. Caspase assay buffer: 10% w/v sucrose, 0.1% w/v CHAPS, 5 mM dithiothreitol, 100 mM HEPES–Tris pH 7.2.
4. RIPA buffer (Sigma).

2.3. Western Blotting

1. Precast 15% SDS-PAGE gel (Bio-Rad).
2. Running buffer(5×): 125 mM Tris, 960 mM glycine, 0.5%(w/v) SDS.
3. Prestained molecular weight marker, Kaleidoscope markers (Bio-Rad).
4. Transfer buffer: 20 mM Tris, 150 mM glycine, 20%(v/v) methanol.
5. Nitrocellulose membrane and chromatography paper (both from Bio-Rad).
6. Tris-buffered saline with Tween(TBS-T) as powdered form (Sigma). Make a 1-L solution with distilled water and store at room temperature.
7. Blocking buffer: 5% (w/v) nonfat dry milk in TBS-T.
8. Antibody dilution buffer: 0.5% (w/v) nonfat dry milk in TBS-T.
9. Primary antibody: Monoclonal anticytochrome *c* (clone 7H8.2C12, BD Pharmingen)
10. Secondary antibody: Antimouse IgG conjugated to horse radish peroxidase (GE healthcare).
11. SuperSignal West Pico chemiluminescent substrate and CLXPosure films (both from Pierce).

2.4. Fluorophores

1. Ratiometric calcium probes: fura/FA (K_d 224 nM, Teflabs or Molecular Probes) and fura2FF/FA (K_d~4 μM, Teflabs) (ex: 340 and 380 nm, em: 535 nm). Make 1 mM stock by dissolving in distilled water. Prepare aliquots and store at −20°C.
2. Ratiometric mitochondrial membrane potential probe JC1 (ex: 570 nm, 490 nm; em: 595 nm, 535 nm) (Molecular Probes). Make 1 mM stock by dissolving in DMSO. Prepare aliquots and store at −20°C.
3. Mitochondrial membrane potential probe TMRE (ex: 540 nm, em: 580 nm) (Molecular Probes). Make 1 mM stock by dissolving in DMSO. Store at −20°C.

4. Fluorogenic caspase substrate: Ac-DEVD-AMC (ex: 380 nm, em: 460 nm) (BD Pharmingen). Reconstitute a stock of 1 mg/mL in DMSO, make aliquots and store at −20°C.

3. Methods

3.1. Simultaneous Measurement of the Ca^{2+}-Induced Changes of $\Delta\Psi_m$ and $[Ca^{2+}]c$ in Suspension of Permeabilized HepG2 Cells

The cytoplasmic free Ca^{2+} concentration ($[Ca^{2+}]_c$) is maintained at about 100 nM, a very low level relative to the extracellular fluid ($[Ca^{2+}]_{EC}\approx1.2$ mM). Temporally and spatially organized increases in $[Ca^{2+}]_c$ and $[Ca^{2+}]_m$ represent one of the most commonly used intracellular signals. However, prolonged changes in Ca^{2+} distribution including an elevation in $[Ca^{2+}]_c$ and $[Ca^{2+}]_m$ trigger a variety of cascades that lead to cell death. The mitochondrial matrix is separated from the cytoplasm by two membranes and the IMM has a very limited permeability to ions. However, conditions of elevated $[Ca^{2+}]_c$ evoke activation of the Ca^{2+} uniporter that mediates a $\Delta\Psi_m$ driven Ca^{2+} uptake to the mitochondria. The uniporter-mediated Ca^{2+} uptake can be effectively inhibited by ruthenium red or by Ru360. Calcium uptake by the mitochondria lowers the $[Ca^{2+}]_c$ and is associated with some, typically transient depolarization. Mitochondrial Ca^{2+} uptake also results in a $[Ca^{2+}]_m$ elevation that is transient under physiological conditions and is central for the activation of the Ca^{2+} -dependent processes of mitochondrial ATP production. However, excess load of Ca^{2+} to the mitochondria leads to the opening of PTP, permeabilization of the IMM for solutes and ions, and the ensuing collapse of Ψm and release of Ca^{2+} to the cytoplasm, referred as delayed Ca^{2+} dysregulation (2, 16). The PTP activation can be blocked by cyclosporin A (CsA) and sanglifehrin A, which bind to CypD and by bongkrekic acid that binds to the ANT (3). Simultaneous measurements of $\Delta\Psi_m$ and $[Ca^{2+}]_c$ allow real-time recording and quantitative analysis of these processes and therefore represent useful means to evaluate the role of mitochondria in Ca^{2+} -dependent cell death (Fig. 2) (7). For monitoring of $\Delta\Psi_m$, a commonly used probe is JC-1, a lipophilic fluorescent cation. JC-1 is present as a green-fluorescent monomer in the cytoplasm. The highly negative $\Delta\Psi_m$ (−180 mV) facilitates the mitochondrial accumulation of JC-1 that in turn, incorporates into the mitochondrial membrane and forms aggregates (J aggregates). This aggregation changes the fluorescence properties of JC-1 leading to a shift from green to orange/red fluorescence. Thus, quantitation of both the mitochondrial red fluorescence and the cytoplasmic green fluorescence provides information on the $\Delta\Psi_m$. JC-1 data is commonly presented as the ratio of the red and green fluorescence, where the ratio is in a direct relationship with the $\Delta\Psi_m$. Calculation of the JC-1 ratio improves the signal and helps to eliminate artifacts that affect both green and red fluorescence but the user has to remember that the green and red fluorescence are originated from two different cellular compartments. For the measurement of $[Ca^{2+}]_c$ a ratiometric Ca^{2+} probe is practical: fura2/FA (if the $[Ca^{2+}]_c$ is <2 μM) or the lower affinity furaFF/FA. Fura-dyes are used in excitation ratio mode (near-UV excitation, ex1: 340 nm, ex2: 380 nm) and the emitted fluorescence can be conveniently measured in the blue-green range. The hydrophilic FA forms are confined to the cytoplasm. While calibration of the JC-1 fluorescence in terms of mV s is very difficult, calibration of the fura ratio in terms of nM $[Ca^{2+}]_c$ can be done by a simple calibration procedure. Also, from changes in the fura ratio evoked by the addition of $CaCl_2$, one can determine the amount of calcium accumulated or released by the mitochondria.

1. Adherent cell cultures were grown to confluency in T75 flasks, then were washed with PBS and harvested by using 0.25% trypsin–EDTA.
2. Harvested cells were washed with ice cold Ca^{2+}-free extracellular buffer (*see* **Subheading 2.2**) and total cell proteins were estimated (by Lowry's method).

3. Equal aliquots of the cell suspension (2.4-mg protein each) were generated and were stored in Ca^{2+}-free extracellular buffer on ice (*see* Note 1).

4. Before using the cell aliquots were centrifuged (150 × *g* for 5 min) and the supernatant was quantitatively removed (*see* Note 2).

5. An aliquot of cells was resuspended in 1.5 mL of ICM (*see* **Subheading 2.2**) and permeabilized with 30–40 μg/mL digitonin in a spectrofluometric cuvette under magnetic stirring at 37°C (*see* Note 3).

6. In order to carry out simultaneous measurements of $[Ca^{2+}]_c$ and $\Delta\Psi_m$, the permeabilized cells were supplemented with 0.5 μM furaFF/FA and 800 nM JC-1 (*see* Note 4).

7. Fluorescence measurements were done in a multi-wavelength-excitation dual wavelength-emission fluorimeter (Delta RAM, PTI) using 340- and 380-nm excitation and 535-nm emission for fura2FF whereas 490-nm excitation/535-nm emission and 570-nm excitation/595-nm emission were used for JC1 (*see* Note 5).

8. After addition of digitonin, furaFF/FA and JC-1 start to record the fluorescence.

9. At 50 s, 2 mM succinate (complex II substrate) or 1 mM/ 5 mM malate/glutamate (complex I substrate) was added to energize the mitochondria.

10. At 100 s, 2 mM MgATP and ATP regenerating system composed of 5 mM phosphocreatine, 5 U/mL creatine kinase was added to provide energy for the ATP-dependent processes (*see* Note 6).

11. After reaching a steady state in the JC-1 ratio, three pulses of $CaCl_2$ (40 μM each) were added in 30-s intervals in the cuvette by a Hamilton syringe during continuous recording. The amount of added $CaCl_2$ was chosen so that the last pulse evoked a reversible depolarization and $[Ca^{2+}]_c$ rise gradually recovering in 2–3 min in the control cells. Both the Ca^{2+}-induced depolarization and the decay of the $[Ca^{2+}]_c$ rise were eliminated if the permeabilized cells were pretreated with ruthenium red (2 μM), an inhibitor of the uniporter (Fig. 2a; *see* Note 7).

12. Stress agents like C2-ceramide (40 μM), which were tested for sensitization of the Ca^{2+}-induced activation of the PTP were added 180 s prior to start the Ca^{2+} pulsing (Fig. 2a)(6, 7, 17).

13. Cyclosporin A (CsA, 5 μM) was added from the start of the recording to clarify the involvement of PTP in the stress agent and Ca^{2+}-induced changes in $\Delta\Psi_m$ and $[Ca^{2+}]$ (Fig. 2b; *see* Note 8).

---

[1]Cell aliquots of different cell types can be stored for 4–12 h without an apparent change in the mitochondrial and ER Ca^{2+} handling and $\Delta\Psi_m$ generation.

[2]EGTA, a Ca^{2+} chelator was present in the cell storage buffer and affected the fura2 fluorescence changes if it was not removed from the cell suspension.

[3]To achieve permeabilization of the plasma membrane in >99% of the cells and to avoid permeabilization of the mitochondrial and ER membranes, the digitonin concentration has to be carefully titrated for each cell type. To determine the lowest effective concentration of digitonin, we used Trypan Blue that only enters the cells upon the loss of the plasma membrane barrier and visualized the blue permeabilized cells under a microscope.

[4]The relatively low affinity of fura2FF for Ca^{2+} ($K_d \sim 4$ μM for fura2FF) was favorable for avoiding saturation of the dye during large increases of $[Ca^{2+}]_c$.

[5]The cuvette chamber was attached with a circulating water bath to maintain 37°C temperature continuously.

[6]Mitochondria that have intact IMM but lack normal respiratory chain activity could generate a $\Delta\Psi_m$ using ATP utilizing the reversed operation of the F1F0-ATP synthase.

[7]Usually less amount of calcium pulsing is required to evoke the similar effect when complex I substrates were used.

[8]CsA targets multiple factors in intact cells but the cytoplasmic targets are largely diluted and effectively eliminated after cell permeabilization. As a negative control, FK506 (5 μM) was used that fails to stabilize the closed state of the PTP but inhibits the cytoplasmic targets of the CsA.

14. After calcium pulsing the recording was continued for at least 5 min and then an uncoupler, FCCP (5 μM) was added to determine the effect of complete dissipation of the $\Delta\Psi_m$ on the JC-1 ratio. In some experiments, a Ca^{2+} ionophore was added prior to FCCP addition to mobilize the total Ca^{2+} that was retained in the mitochondria and ER.

15. Calibration of the furaFF signal was carried out at the end of each measurement adding 1.5 mM $CaCl_2$ and subsequently 10 mM EGTA–Tris pH 8.5. $[Ca^{2+}]_2$ was calculated by using a K_d of 4 μM. Increases of cytosolic $[Ca^{2+}]$ obtained by addition of $CaCl_2$ were calculated using constants obtained from (18).

16. In most measurements, thapsigargin, an inhibitor of the SERCA Ca^{2+} pump (2 μM) was included to abolish the ER Ca^{2+} uptake so the added Ca^{2+} was accumulated only by the mitochondria. However, in some experiments thapsigargin was omitted and the ER was preloaded by mini pulses of Ca^{2+} (1 μM each) and then ER Ca^{2+} release was induced by IP3. Due to a local Ca^{2+} transfer between mitochondria and adjacent ER, Ca^{2+} release through the IP3 receptor was very effectively relayed to the mitochondria and caused PTP opening in cells exposed to some stress agents (e.g., C2).

3.2. Fluorometric Measurement of the tBid-Induced Loss of $\Delta\Psi_m$ in Suspension of Permeabilized HepG2 and H9c2 Cells

In response to engagement of the death receptors, procaspase-8 is activated to cleave Bid, a BH3-only Bcl-2 family protein, generating truncated C-terminus Bid (tBid). Recent data showed that the cleavage and the ensuing activation of Bid can also be catalyzed by several enzymes including calpain, caspases, cathepsins, and granzyme B in various cell death paradigms (19). tBid interacts with the mitochondria to cause permeabilization of the OMM and subsequent release of proteins from the IMS, which mediate the execution of apoptosis. The tBid-induced OMM permeabilization depends on interplay between pro- and antiapoptotic Bcl-2 family proteins in the OMM (Bak, Bax, and Bcl-xL) and involves cardiolipin but the exact mechanism remains unclear. During tBid-induced release of apoptotic factors from the mitochondria, the inner IMM barrier function is maintained in several experimental models, although remodeling of the cristae seems to be necessary to allow the discharge of the IMS proteins. The IMS protein, cytochrome *c* is necessary for the mitochondrial electron transport chain function and upon release to the cytoplasm, induces caspase activation in the apoptosome. Thus, if $\Delta\Psi_m$ generation was due to the electron transport chain activity, release of cytochrome *c* from the mitochondria to the cytosol appears as mitochondrial depolarization (20). This process was monitored by various potentiometric fluorophores (JC-1, tetramethylrhodamine ethyl esters (TMRE), tetramethylrhodamine methyl esters (TMRM), and Rhodamine123 (R123)) in permeabilized HepG2 and H9c2 cells. Fluorometric recording of $\Delta\Psi_m$ by JC-1 has been described (*see* **Subheading 3.1**). All the other probes are also cationic fluorophores that are accumulated in the mitochondria in proportion to the $\Delta\Psi_m$, These dyes do not form aggregates in the membranes and interact with membrane proteins minimally and thus are preferred probes for quantitative measurements of the membrane potential using Nernst equation. However, if these probes are present in the cytoplasm at micromolar concentration, accumulation in the mitochondria leads to quenching of their fluorescence. Mitochondrial depolarization due to cytochrome *c* release or to uncoupling appeared as dequenching of the TMRE, TMRM, or R123 fluorescence (*see* Fig. 3). However, the tBid-induced dequenching was dependent on the presence of oligomycin, an inhibitor of the F1F0 ATPase, indicating that the ATP synthase function in the reverse mode was competent to maintain the $\Delta\Psi_m$ despite the release of cytochrome *c* and other IMS proteins (*see* Fig. 3a). This result was an evidence that tBid does not interfere with the IMM barrier function. While the tBid effect on the $\Delta\Psi_m$

was recorded in the fluorometer, at any time points, aliquots of the permeabilized cell suspension can be obtained and rapidly processed for separation of cytosol and membrane fractions that can be used for biochemical or fluorometric detection of the distribution of the mitochondria-derived apoptotic factors (*see* **Subheading 3.4**) (20). The protocol for the fluorometric measurement of TMRE is as follows:

1. **Steps 1–5** were the same as in **Subheading 3.1**.
2. For measurements of $\Delta\Psi_m$, the permeabilized cells were supplemented with 2 μM TMRE.
3. Fluorescence measurement was done in the same fluorometer described in **Subheading 3.1** using 540-nm excitation and 580-nm emission.
4. **Step 8–10** were the same as above.
5. At 150 s 2.5- μg/mL oligomycin was also added to prevent the function of the mitochondrial F1F0 ATPase.
6. At 300 s recombinant tBid was added. tBid could be added at different concentration to establish a dose–response relationship for the OMM-permeabilization.
7. FCCP (5 μM) was added at the end of each run to achieve complete depolarization of the mitochondria.

3.3. The Ca^{2+} and tBid-Induced Changes in Mitochondrial Volume with Time as Monitored by Light Scattering in Permeabilized HepG2 and H9c2 Cells

Under conditions of prolonged opening of the PTP (e.g., Ca^{2+} overload), the mitochondrial matrix volume increases. By contrast, selective permeabilization of the OMM by tBid results in no change or a decrease in matrix volume. Therefore, measurement of the mitochondrial volume may provide some clues to the mechanism of the mitochondrial membrane permeabilization. As mitochondria swell, their refractive index decreases, yielding a drop in light absorbance at higher wavelengths. Monitoring 90° light scatter in mitochondrial suspensions has been commonly used to evaluate changes in mitochondrial volume. Light scattering is usually measured at 520 nm, an isosbestic point for the mitochondrial cytochromes and thus insensitive to changes in redox state. Importantly, light scattering can be monitored simultaneously with the measurement of $[Ca^{2+}]_c$ or $\Delta\Psi_m$. The absolute values for A_{520} are dependent on several factors in addition to the matrix volume, including the concentration of the mitochondria and the optical geometry of the fluorometer. In addition, light scattering is sensitive to changes in the shape and the IMS of the mitochondria (21, 22). Therefore, light scattering measurements can be used to assess the rate of change of matrix volume but do not allow determination of absolute values. Measurement of mitochondrial volume in permeabilized cells is further complicated by the contribution of other organelles to the light scatter. To test the contribution of mitochondrial volume to the changes in light scatter pharmacological means can be used. For example, CsA prevents the Ca^{2+} -induced decrease of absorbance in permeabilized cells (*see* Fig. 2c), providing an evidence for PTP-mediated mitochondrial swelling.

3.4. Separation of Cytosolic Fraction and Western Blot Analysis

Both the Ca^{2+} -induced PTP opening and the tBid-induced OMM permeabilization of mitochondria commit the cell to apoptosis by stimulating the release of apoptosis promoting factors to the cytoplasm. These are mitochondrial IMS proteins like cytochrome *c*, AIF, Smac/DIABLO, OMI/HtrA2, pro-caspases, etc. which are involved in the formation of apoptosome or initiate other apoptosis executing mechanisms (3). To quantitate the release

of the IMS proteins, the permeabilized cell suspensions have to be rapidly fractionated in the end of the fluorometric measurements. The mitochondria containing membrane fraction can be separated from the cytoplasm by a centrifugation protocol in 5 min. Furthermore, a rapid filtration-based protocol has also been set up, which allows one to obtain mitochondria-free cytoplasm in 5 s (17). To assess the time course of the release of IMS proteins relative to changes in $\Delta\Psi_m$ and $[Ca^{2+}]_c$, cell samples can be obtained and filtered at multiple time points during the fluorometric measurement. Western blotting of the cytosolic and membrane fractions provides a simple approach to evaluate the release of each IMS protein (*see* Fig. 4a–d). The detailed method for separation of cytosolic and membrane fractions and Western blotting of cytochrome *c* is as follows:

1. After completion of the fluorometric measurement of $\Delta\Psi_m$ and $[Ca^{2+}]_c$ the cell suspension was rapidly centrifuged at 12,000 × *g* for 5 min (*see* Note 9).
2. Alternatively, the cell suspension was rapidly passed through a syringe-less filter device (Autovial, 0.45- μm cellulose acetate membrane, Whatman) that retains the cellular membranes.
3. The supernatant (cytoplasm) and pellet (cellular membranes) produced by the centrifuge approach and the flow-trough generated by the filtration were put immediately in liquid nitrogen for rapid freezing. Subsequently, the samples were stored at −80°C.
4. Membrane fractions separated by centrifugation was lyzed by RIPA buffer. The membranes were incubated for 40 min in 4°C by rotating it and then centrifuged for 15 min in 12,000 × *g*. Supernatant were saved at −80°C for future use.
5. Proteins (25 μg) were separated by SDS-PAGE (15% gel) under reducing condition.
6. Separated proteins were transferred to nitrocellulose membrane.
7. Blocked the membrane in blocking buffer overnight in 4°C with gentle shaking.
8. Next morning washed the membrane with TBS-T in room temperature with shaking for 5 min.
9. The membrane was incubated with the primary antibody (anticytochrome *c*) at 1:500 dilutions in antibody dilution buffer with gentle shaking for 5 h in room temperature.
10. The membrane was washed with TBS-T in room temperature with shaking for six times with 5 min duration for each washing cycle.
11. The membrane was incubated in secondary antibody at 1:5,000 dilutions in antibody dilution buffer and was shaken gently for 1.5 h at room temperature.
12. The membrane was washed with TBS-T in room temperature with shaking for six times for 5 min for each washing cycle.
13. The blots were taken to the darkroom and were developed using an enhanced chemiluminescence kit.

[9]It is recommended that the samples are centrifuged at 4°C but the cytochrome *c* distribution did not seem to be altered when centrifuging was done at room temperature.

3.5. Caspase Assay

The mitochondrial phase of apoptosis involves the release of apoptosis promoting proteins from the mitochondria and the assembly of the apoptosome. Here, cytochrome *c* binds Apaf-1 and in the presence dATP or ATP, recruits and activates procaspase-9 to form a complex that initiates activation of the effector caspases (e.g., caspase-3). The ICE family member Caspase-3 is involved in proteolysis of several important proteins including poly (ADP ribose) polymerase (PARP). The caspase-3-specific cleavage site is formed by DEVD that has also provided a sequence for generation of an artificial peptide substrate. Binding of the DEVD peptide to a fluorophore is utilized for an in vitro assay of caspase-3 activity. For example, when caspase-3 is incubated with Ac-DEVD-aminomethylcoumarin (AMC), the active caspase-3 cleaves the tetrapeptide between D and AMC, thus releasing fluorogenic AMC that can be measured in a fluorometer (ex: 380 nm, em: 460 nm). The detailed protocol of measuring caspase-3 activity in the cytoplasm fractions (*see* **Subheading 3.4**) is described below (*see* Fig. 4e, f).

1. 180-μL of cytoplasmic extract (protein concentration: 0.8– 1.2 mg/mL) was added to 1,420 μL of caspase assay buffer in a cuvette.
2. The mixture was incubated for 10 min at 37°C and then the recording of fluorescence.
3. Add 12.5 μM substrate, Ac-DEVD-AMC, into the mixture and take another reading.
4. Assay mixture was incubated in the presence of substrate for 30 min at 37°C and the fluorescence of free AMC (ex: 380 nm, em: 460 nm) was monitored using the fluorometer described above.
5. Addition of exogenous cytochrome *c* (400 nM) to the assay mixture brought about a large increase in DEVD-AMC cleavage proved the requirement of cytochrome *c* for activation of Caspase 3.
6. Fluorescence was also measured in samples that did not contain any cytosol or were incubated in the presence of a caspase inhibitor. The results were used to make correction for the noncaspase-dependent increase in AMC fluorescence. Furthermore, the fluorescence of various amounts of free AMC was also measured to establish the AMC vs. fluorescence relationship and to calculate the number of DEVD-AMC molecules cleaved by the effector caspase enzymes.

Acknowledgments

We would like to thank Drs. György Csordás, Gábor Szalai, Xuena Lin, Muniswamy Madesh, Cecilia Garcia, Ludivine Walter, and Mrs. Erika Davies for their dedicated efforts in setting up the approaches described here. This work was supported by R01-GM59419 from the National Institutes of Health to G.H.

References

1. Duchen MR. Mitochondria in health and disease: perspectives on a new mitochondrial biology. Mol Aspects Med. 2004; 25:365–451. [PubMed: 15302203]
2. Rizzuto R, Pozzan T. Micro-domains of intracellular Ca^{2+}: molecular determinants and functional consequences. Physiol Rev. 2006; 86:369–408. [PubMed: 16371601]
3. Kroemer G, Galluzzi L, Brenner C. Mitochondrial membrane permeabilization in cell death. Physiol Rev. 2007; 87:99–163. [PubMed: 17237344]
4. Chipuk JE, Bouchier-Hayes L, Green DR. Mitochondrial outer membrane permeabilization during apoptosis: the innocent bystander scenario. Cell Death Differ. 2006; 13:1396–1402. [PubMed: 16710362]

5. Bernardi P, Forte M. The mitochondrial permeability transition pore. Novartis Found Symp. 2007; 287:157–164. discussion 164–159. [PubMed: 18074637]
6. Hajnoczky G, Davies E, Madesh M. Calcium signaling and apoptosis. Biochem Biophys Res Commun. 2003; 304:445–454. [PubMed: 12729578]
7. Szalai G, Krishnamurthy R, Hajnoczky G. Apoptosis driven by IP(3)-linked mitochondrial calcium signals. EMBO J. 1999; 18:6349–6361. [PubMed: 10562547]
8. Scorrano L, Penzo D, Petronilli V, Pagano F, Bernardi P. Arachidonic acid causes cell death through the mitochondrial permeability transition. Implications for tumor necrosis factor-alpha aopototic signaling. J Biol Chem. 2001; 276:12035–12040. [PubMed: 11134037]
9. Adams JM, Cory S. Bcl-2-regulated apoptosis: mechanism and therapeutic potential. Curr Opin Immunol. 2007; 19:488–496. [PubMed: 17629468]
10. Kuwana T, Newmeyer DD. Bcl-2-family proteins and the role of mitochondria in apoptosis. Curr Opin Cell Biol. 2003; 15:691–699. [PubMed: 14644193]
11. Danial NN, Korsmeyer SJ. Cell death: critical control points. Cell. 2004; 116:205–219. [PubMed: 14744432]
12. Antignani A, Youle RJ. How do Bax and Bak lead to permeabilization of the outer mitochondrial membrane? Curr Opin Cell Biol. 2006; 18:685–689. [PubMed: 17046225]
13. Luo X, Budihardjo I, Zou H, Slaughter C, Wang X. Bid, a Bcl2 interacting protein, mediates cytochrome *c* release from mitochondria in response to activation of cell surface death receptors. Cell. 1998; 94:481–490. [PubMed: 9727491]
14. Wei MC, Lindsten T, Mootha VK, Weiler S, Gross A, Ashiya M, Thompson CB, Korsmeyer SJ. tBID, a membrane-targeted death ligand, oligomerizes BAK to release cytochrome. c Genes Dev. 2000; 14:2060–2071.
15. Scorrano L, Ashiya M, Buttle K, Weiler S, Oakes SA, Mannella CA, Korsmeyer SJ. A distinct pathway remodels mitochondrial cristae and mobilizes cytochrome *c* during apoptosis. Dev Cell. 2002; 2:55–67. [PubMed: 11782314]
16. Hajnoczky G, Csordas G, Das S, Garcia-Perez C, Saotome M, Sinha Roy S, Yi M. Mitochondrial calcium signalling and cell death: approaches for assessing the role of mitochondrial Ca^{2+} uptake in apoptosis. Cell Calcium. 2006; 40:553–560. [PubMed: 17074387]
17. Madesh M, Hajnoczky G. VDAC-dependent permeabilization of the outer mitochondrial membrane by superoxide induces rapid and massive cytochrome *c* release. J Cell Biol. 2001; 155:1003–1015. [PubMed: 11739410]
18. Bers DM, Patton CW, Nuccitelli R. A practical guide to the preparation of Ca^{2+} buffers. Methods Cell Biol. 1994; 40:3–29. [PubMed: 8201981]
19. Yin XM. Bid, a BH3-only multifunctional molecule, is at the cross road of life and death. Gene. 2006; 369:7–19. [PubMed: 16446060]
20. Madesh M, Antonsson B, Srinivasula SM, Alnemri ES, Hajnoczky G. Rapid kinetics of tBid-induced cytochrome *c* and Smac/DIABLO release and mitochondrial depolarization. J Biol Chem. 2002; 277:5651–5659. [PubMed: 11741882]
21. Das M, Parker JE, Halestrap AP. Matrix volume measurements challenge the existence of diazoxide/glibencamide-sensitive KATP channels in rat mitochondria. J Physiol. 2003; 547:893–902. [PubMed: 12562892]
22. Petronilli V, Cola C, Massari S, Colonna R, Bernardi P. Physiological effectors modify voltage sensing by the cyclosporin A-sensitive permeability transition pore of mitochondria. J Biol Chem. 1993; 268:21939–21945. [PubMed: 8408050]

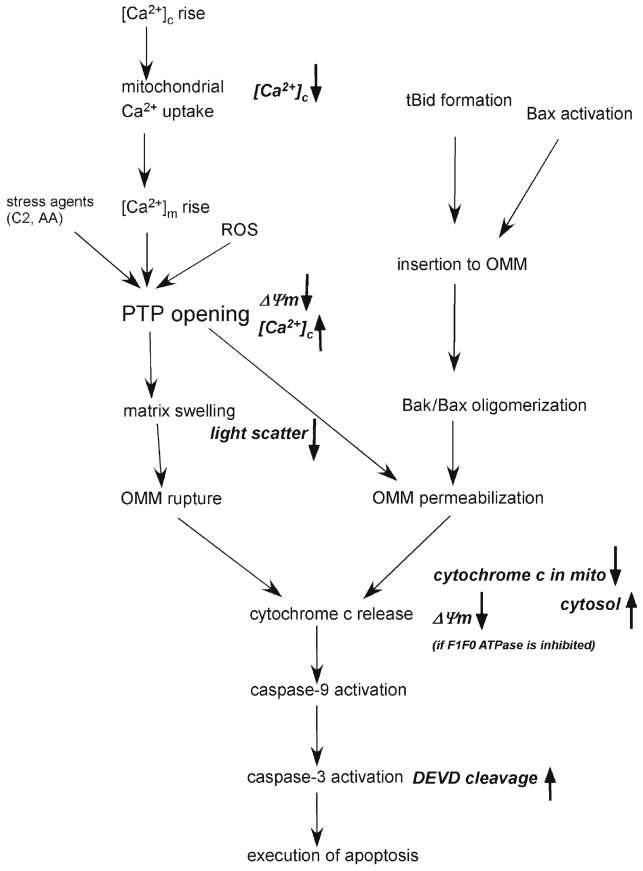

Fig. 1.

Mitochondrial phase of apoptosis: mechanisms and measurements. Mechanisms of the mitochondrial phase of calcium and tBid/Bax-dependent apoptosis are depicted in *black*. The parameters measured by the presently described fluorometric approaches are shown in *italics*. *C2* C2-ceramide, *AA* Arachidonic acid.

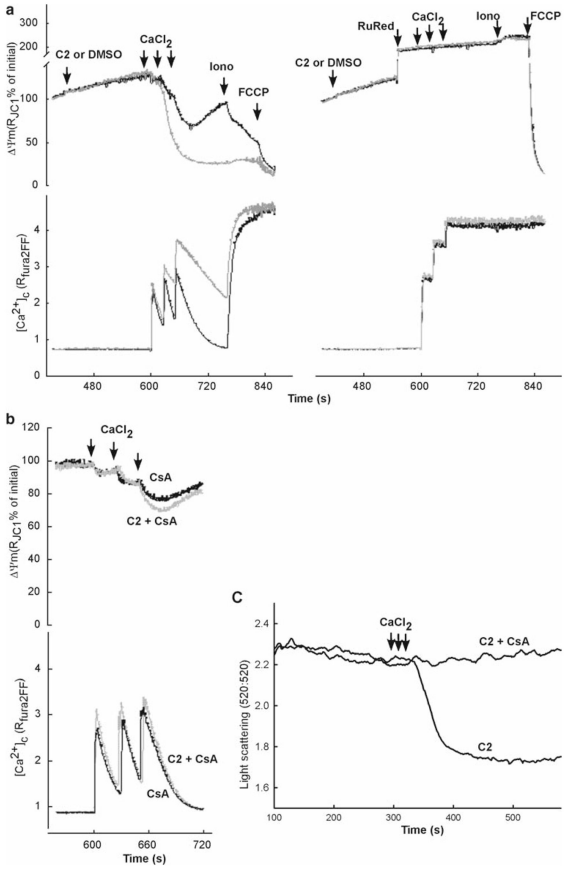

Fig. 2.

Ca^{2+}-induced $\Delta\Psi_m$, $[Ca^{2+}]_c$ and mitochondrial swelling responses in permeabilized HepG2 cells exposed to proapoptotic stimuli. (**a**) Simultaneous measurements of $\Delta\Psi_m$ and $[Ca^{2+}]_c$ were carried out in suspensions of permeabilized cells using a membrane potential probe, JC1, and a Ca^{2+} tracer, fura2FF, respectively. Permeabilized cells were treated with C2 or DMSO 180 s prior to the addition of Ca^{2+} pulses. Representative analog traces (*black* – control and *gray* – C2) in the *left panel* shows the C2-induced enhancement of the $\Delta\Psi_m$ loss and $[Ca^{2+}]_c$ rise (referred as delayed Ca^{2+} dysregulation). *Right panel* shows the same measurements in the presence of ruthenium red (2 μM RuRed added 60 s prior to Ca^{2+}). As RuRed blocks the mitochondrial Ca^{2+} uptake, it protects the cells from the C2-induced enhancement of the $\Delta\Psi_m$ loss and $[Ca^{2+}]_c$ rise. (**b**) To establish the role of PTP, similar measurements were carried out in presence of CsA. Blocking of C2-induced enhancement of the $\Delta\Psi_m$ loss and $[Ca^{2+}]_c$ rise by CsA indicate the involvement of PTP in the process of C2-induced delayed Ca^{2+} dysregulation. (**c**) Simultaneous measurements of light scattering and $[Ca^{2+}]_c$ were carried out in suspensions of permeabilized HepG2 cells in presence of C2 only or C2 + CsA. In presence of C2, rise of $[Ca^{2+}]_c$ activates PTP opening and simultaneous swelling of mitochondria which is detected by the drop of the light scattering. CsA prevents PTP opening and protects mitochondria from C2 + Ca^{2+} -induced swelling. Panels (**a**) and (**b**) are reproduced from (7) with modification with permission from *The EMBO Journal*

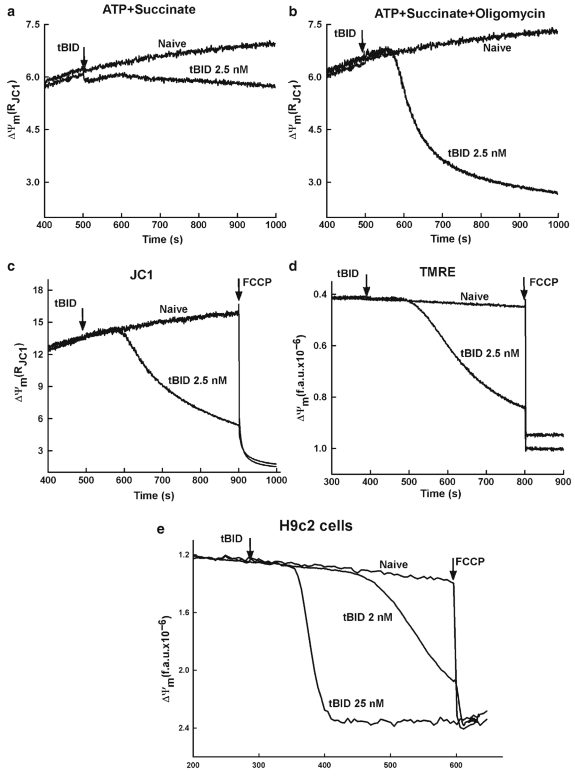

Fig. 3.

tBid-induced OMM permeabilization and subsequent $\Delta\Psi_m$ loss in permeabilized cells. *Upper panel* shows the measurements of $\Delta\Psi_m$ using JC1 in permeabilized HepG2 cells incubated in the presence of succinate, ATP, and ATP regenerating system (**a**) succinate, ATP, ATP regenerating system, and oligomycin (**b**). As shown in (**a**), permeabilized cells supplied with succinate (complex II substrate) and ATP regenerating system (ATP, creatine phosphate, and creatine phosphokinase) in the absence of oligomycin showed relatively small tBid-induced depolarization. Addition of oligomycin augmented tBid-induced depolarization (**b**), suggesting that $\Delta\Psi_m$ was maintained after cytochrome *c* release utilizing extramitochondrial ATP in the reverse function of the F_1F_0 ATPase. *Middle panel* shows the comparative measurements of $\Delta\Psi_m$ using JC1 (**c**) and TMRE (**d**) in permeabilized HepG2 cells incubated in the presence of succinate, ATP, ATP regenerating system, and oligomycin. tBid causes a decreases of the JC1 ratio (**c**) and an increase in TMRE fluorescence, reflecting the release of TMRE from the depolarized mitochondria (**d**). The time course of TMRE dequenching is very similar to the decrease in JC1 ratio providing the evidence that both of these dyes could be used for efficient detection of tBid-induced $\Delta\Psi_m$ loss. In the *lower panel,* $\Delta\Psi_m$ was monitored using TMRE in permeabilized H9c2 cells treated with two different doses of tBid (**e**) for 5 min. The loss of $\Delta\Psi_m$ after treatment with tBid exhibited both a dose-dependent lag time of response and a lower rate of depolarization. Panels (**a**)–(**d**) are reproduced from (20) with modification with permission from *The Journal of Biological Chemistry*

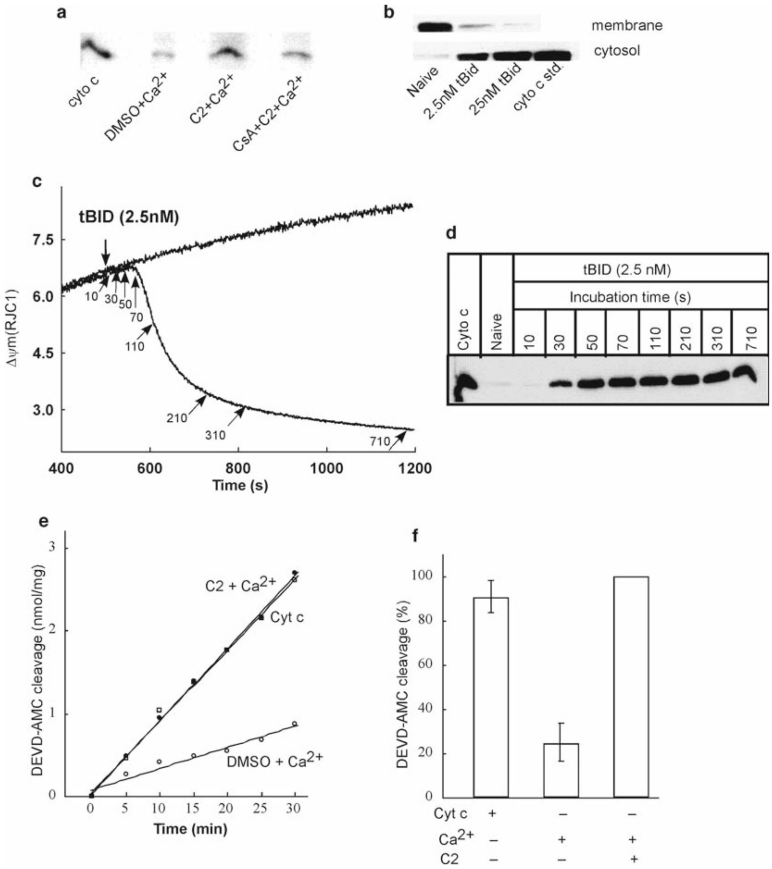

Fig. 4.

Release of cytochrome *c* and activation of caspases after $\Delta\Psi_m$ loss in permeabilized HepG2 cells. *Upper panel* shows the immunoblots of cytochrome *c* in cytosolic and membrane fractions generated after the measurements of $\Delta\Psi_m$ in permeabilized cells. Cytosolic samples generated from the experiments described in Fig. 2a, b shows higher amount of cytochrome *c* in presence of C2 + Ca^{2+} compared to that of C2 + Ca^{2+} + CsA reflecting PTP opening (**a**). Membrane and cytosolic samples generated after $\Delta\Psi_m$ measurements in presence of two different concentrations of tBid shows dose-dependent release of cytochrome *c* in cytosol from the mitochondria (**b**). *Middle panel* shows that tBid-induced $\Delta\Psi_m$ loss is closely coupled to cytochrome *c* release. $\Delta\Psi_m$ was monitored in permeabilized cells treated with 2.5 nM tBid in the presence of succinate, ATP, ATP regenerating system, and oligomycin. *Arrows* indicate the time points at which cytosolic samples were generated by rapid filtration of the cells (**c**). Panel (**d**) shows time course of tBid-induced cytochrome *c* release as determined by Western blotting of the cytosolic samples. *Lower panel* shows caspase activation associated with Ca^{2+} -induced opening of PTP. Fluorometric assay of DEVD–AMC cleavage in cytosol extracts prepared at the end of measurements of $\Delta\Psi_m$ (*see* Fig. 2a) was carried out. Data in (**e**) shows the increase of Caspase 3 activity in presence of C2 + Ca^{2+} compared to DMSO control. Addition of exogenous cytochrome *c* in DMSO control cytosol increased its activity of Caspase 3 at the level of C2 + Ca^{2+} condition indicate that activation of Caspase 3 is downstream to the cytochrome *c* release. Data in (**f**) shows the DEVD-AMC cleavage normalized to the activity obtained with C2 + Ca^{2+}. Panels (**a**) and (**e**) are reproduced from (7) with modification with permission from *The EMBO Journal*, whereas panels (**c**) and (**d**) from (20) with modification with permission from *The Journal of Biological Chemistry*